14º ENCONTRO BRASILEIRO SOBRE ADSORÇÃO
23 A 25 DE NOVEMBRO DE 2022

ZnAl/LDH adsorbents for Congo Red and Methyl Orange Dyes Removal

Larissa Farias Queiroz[a], Icaro Mychel Gomes Leite de Sa[a], Pollyanna Vanessa dos Santos Lins[a], Thais Logetto Caetité Gomes[a], Lucas Meili[a*]

[a] *Laboratorio de Processos (LaPro), Centro de Tecnologia, Universidade Federal de Alagoas, Avenida Lourival Melo Mota, Maceio 57072-900, Brazil*

Abstract: This work aimed to investigate the adsorption capacity of the ZnAl/LDH to remove methyl orange and congo red dyes from aqueous solution. The absorbent characterization indicated typical morphological and structural properties characteristic of layered double hydroxides. From the absorption tests, it was possible to verify that the solution's pH did not significantly affect the adsorptive process for the two pollutants. The kinetic study presented a better adjustment for the pseudo-first-order model, indicating physisorption as the major mechanism for the adsorption of the two dyes studied. Finally, a removal percentage of 99.1% was achieved for congo red, and 96.7% for the methyl orange, showing that MgAl/LDH is a promising material in adsorption processes with dyes.
Keywords: Adsorption, LDH, methyl orange; congo red.

1. Introduction

Among the group of minerals referred to as non-silicate oxides and hydroxides, the layered double hydroxides (LDH) have many physical and chemical properties similar to those of clay minerals, also known as “anionic clays” that have a similar structure to brucite [1, 2].

In recent years, there has been an increasing interest in layered double hydroxides (LDHs), due to its great potential as an adsorbent, which may be associated with its lamellar structure, high porosity, high specific surface area, and great chemical and mechanical stability. In addition, due to their properties, LDH can be applied in catalysts and catalyst supports [3], anion exchangers [4], bioactive nanocomposites [5], electroactive and photoactive materials [6], and flame retardant nanocomposites [7].

The Brazilian Health Regulatory Agency (Anvisa) regulates the use of natural and synthetic dyes in the textile and food industry. Synthetic dyes are acquired through organic synthesis. There are several types of dyes, however, the main ones are azo, anthraquinone, heterocyclic, triphenylmethane, and polymeric [8]. Among the organic dyes produced in the world, the azo group (-N=N-) which represents approximately 70% of its totality. Thus, the exacerbated use of these dyes and their environmental disposal generate a great concern, due to their persistence and toxicity. They are accumulated in organisms through metabolism, after ingestion, especially aromatic amines, which have chronic toxicity, with carcinogenic effects [9, 10].

Dyes that have azo bonds (-N=N-) next to the aromatic structure present high stability to photochemical processes and also to degradation by natural factors, implying considerable difficulty in the process of removing it in wastewater [11, 12].

Adsorption is a process that has been extensively studied and used in the treatment of effluents, due to its low operating cost and high efficiency in removing contaminants. Therefore, the use of LDH is a promising alternative for the removal of these dyes in effluent treatment, through the adsorption process.

2. Materials and Characterization

The syntheses were carried out using the coprecipitation method at increasing pH, in a 3:1 molar ratio of ZnAl [1]. The adsorbent was characterized by X-ray diffraction (XRD) was performed in a diffractometer Rigaku Minifex, model 300, applying as radiation Cu-Kα with λ=1.5418 Â. The surface morphology was evaluated by Scanning electron microscopy (SEM, VEGA3 TESCAN). Thermogravimetric analysis (TG/DTG) was performed on a Shimadzu thermobalance, model DTG-60H, where alumina crucibles and sample masses of approximately 10 mg were used. A heating rate of 10 ºC.min^{-1} was used, from room temperature to 800 ºC, in a synthetic air atmosphere with a flow rate of 50 mL.min^{-1}.

2.1. Adsorbate preparation

Two standard solutions were prepared with 200 mg.L^{-1} of methyl orange and congo red as adsorbates. The analytical curve was performed via molecular absorption spectrophotometry in the ultraviolet region through a spectrophotometer

Multispec-1501, Shimadzu. For this, the wavelengths of 464 nm and 498 nm were used for methyl orange and Congo red, respectively [13-15].

2.2. Adsorption tests

The adsorption capacity q_t (mg.g^{-1}) was calculated by Eq. 1.

$$q_t = \frac{(c_o - c_e)}{m} V \quad (1)$$

Where c_o represents the initial concentration of adsorbate (mg.L^{-1}), c_e is the equilibrium concentration (mg.L^{-1}), V is the sample volume (L), and m is the adsorbent mass (g).

2.3. Effect of the solution's initial pH

To determine the pH effect on the adsorption process, solutions with pH values of 4, 5, 6, 7, 8, and 9 were used. Thus, the experiments were conducted under the following conditions: adsorbent mass of 0, 1 g, solution volume of 50 mL, dye concentration of 20 mg.L^{-1}, contact time of 14 h, stirring at 150 rpm, and ambient temperature. The appropriate pH adjustments were performed using 0.1 mol.L^{-1} HCl and 0.1 mol.L^{-1} NaOH solution.

2.4. Kinetics of adsorption

Based on the data obtained in the study of the solution's pH effect, other experiments were carried out without adjusting the solution pH value. Thus, the adsorption was performed with the same conditions of the pH test, varying the time, in the adsorption conditions of 20 mg.L-1 and 5 mg.L-1. Kinetic adsorption was evaluated through pseudo-first-order and pseudo-second-order models. The kinetic adsorption was evaluated according to well-documented procedures [35–37]. The traditional kinetics models were chosen to be fitted to the experimental data. The pseudo-first order (PFO) (Eq.2), and pseudo-second order (PSO) (Eq. 3).

$$q_t = q_1 (1-\exp(-k_1 t)) \quad (2)$$

$$q_t = \frac{t}{\left(\frac{1}{k_2 q_2^2}\right) + \left(\frac{t}{q_2}\right)} \quad (3)$$

Where, k_1 (min^{-1}), and k_2 (g mg^{-1} min^{-1}) for the PFO, PSO, respectively; and q_1, and q_2 are the theoretical adsorption capacities (mg g-1) for the PFO, PSO, models, respectively.

3. Results and discussion

3.1. Characterization

Fig. 1 a) corresponds to the TG/DTG curves in LDH. The results show two regions of huge mass loss. The first one is below 300 °C, in which initially the loss of water occurs in the interlamellar space at between 135-200° C, and between 200-300°C the mass loss can be attributed to dehydroxylation of the structure and decomposition of nitrate anions [16]. The second mass loss occurs between approximately 400-700°C, corresponding to the amount of CO_2 released from the decomposition of carbonates [17,18].

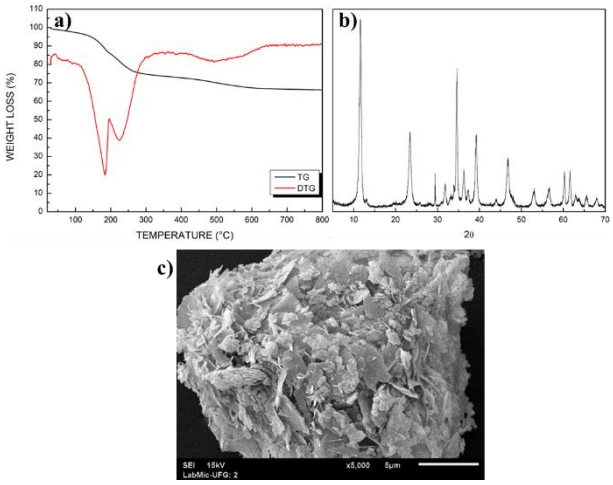

Fig. 1. Adsorbent characterization a) thermogravimetric analysis (TG/DTG), b) X-ray diffraction (XRD), and c) scanning electron microscopy (SEM).

Through Fig. 1 b), it is possible to note that the adsorbent presented peaks at approximately 11.8°; 23.4°; 34.4°, 39.2°, 46.7°, 60°, and 61.7°, which correspond to the reflections (003), (006), (012), (015), (018), (110), and (113), respectively. The results obtained are in agreement with the work of Rodriguez-Rivas et al. [19].

According to Fig. 1 c), it can be seen that the material studied exhibits a regular hexagonal platelet morphology and lamellar structure [20]. The morphology of the material presents characteristics attributed to LDH, dense material with an apparently layered structure, rough surface, and possibly

crystalline structure like sheets. Hexagonal platelets can be attributed to carbonated brucite-like leaves [21].

3.2. Kinetics of adsorption

In Fig. 2. are presented the adsorption kinetics for methyl orange and congo red dyes. From the kinetic studies, it is possible to note that in both pollutants, at a concentration of 20 mg.L^{-1}, the equilibrium is reached in approximately 5 minutes. For a concentration of 50 mg.L^{-1}, the equilibrium is reached in approximately 30 minutes. This time difference was expected since at higher concentrations, there are high adsorption rates at the beginning, which decrease with the occupation of the adsorption sites, thus reducing the adsorption rate. Furthermore, repulsive forces can occur between the adsorbed and non-adsorbed molecules, reducing the time the system needs to reach equilibrium.

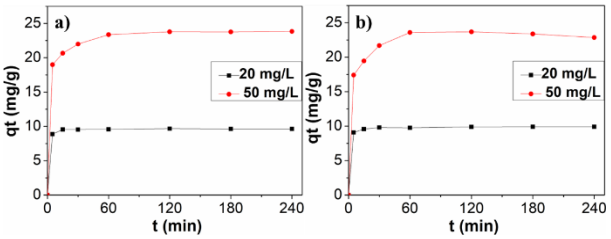

Fig. 2. Adsorption kinetics for a) methyl orange, and b) congo red dyes.

Table 1 shows the data obtained from the adjustments of the pseudo-first-order (PFO) and pseudo-second-order (PSO) kinetic models for methyl orange (MO) and Congo red (CR).

Table 1. Data obtained from the fits of the pseudo-first-order and pseudo-second-order models.

	Model	q_e (mg. g^{-1})	k_{PPO}, k_{PSO}	R^2	ε (%)
MO 20	PFO	9.60	0.5159	0.9998	0.37
(mg L^{-1})	PSO	9.50	-28336	0.9941	1.93
MO 50	PFO	22.95	0.3407	0.9827	4.04
(mg L^{-1})	PSO	22.34	-56274	0.9529	7.15
CR 20	PFO	9.81	0.5205	0.9990	0.82
(mg L^{-1})	PSO	10.00	-41721	0.9936	2.24
CR 50	PFO	22.58	0.2752	0.9742	4.96
(mg L^{-1})	PSO	21.72	-94390	0.9217	9.24

Based on the values of correlation coefficient (R^2) and average relative error (ε), it is possible to observe a better convergence between the experimental data and the pseudo-first-order model. Furthermore, the experimental q_e value is in agreement with the q_e values obtained by fitting the pseudo-first-order model. These conditions were observed for the two pollutants and in the two concentrations studied, thus indicating that the adsorption process occurs mainly via physisorption.

4. Conclusions

From the study, it was possible to conclude that the solution's pH solution did not significantly affect the adsorptive process for the two pollutants, indicating the possibility of its use in a wide pH range. Furthermore, it was observed from the kinetic study that equilibrium was reached between 5 and 30 minutes, with better adjustments for the pseudo-first-order model, indicating physisorption as the major mechanism for the adsorption of the two dyes at the two concentrations studied. Finally, a removal percentage of 99.1% was achieved for congo red, and 96.7% for the methyl orange, showing that ZnAl/LDH is a promising material in adsorption processes with dyes.

References

[1] Forano, C. et al. Layered double hydroxides. Developments in clay science, v. 1, p. 1021-1095, 2006.

[2] Menezes, Janaína et al. Layered double hydroxides (LDHs) as carrier of antimony aimed for improving leishmaniasis chemotherapy. Applied Clay Science, v. 91, p. 127-134, 2014.

[3] Mckenzie, Andrew L.; Fishel, Christopher T.; Davis, Robert J. Investigation of the surface structure and basic properties of calcined hydrotalcites. Journal of Catalysis, v. 138, n. 2, p. 547-561, 1992.

[4] Tagaya, Hideyuki et al. Intercalation of colored organic anions into insulator host lattices of layered double hydroxides. Microporous Materials, v. 7, n. 2-3, p. 151-158, 1996.

[5] Leroux, Fabrice; Besse, Jean-Pierre. Polymer interleaved layered double hydroxide: a new emerging class of nanocomposites. Chemistry of Materials, v. 13, n. 10, p. 3507-3515, 2001.

[6] Giannelis, Emmanuel P.; Nocera, Daniel G.; Pinnavaia, Thomas J. Anionic photocatalysts supported in layered double hydroxides: intercalation and photophysical properties of a ruthenium complex anion in synthetic hydrotalcite. Inorganic Chemistry, v. 26, n. 1, p. 203-205, 1987.

[7] Wang, Zhenyu; HAN, Enhou; Ke, Wei. Influence of nano-LDHs on char formation and fire-resistant properties of flame-retardant coating. Progress in Organic Coatings, v. 53, n. 1, p. 29-37, 2005.

[8] Kieling, A. G; Moraes, C. A. M; Brehm, F. A; Utilização De Cinza De Casca De Arroz Na Remoção De Cromo Hexavalente. Estudos Tecnológicos - Vol. 5, n° 3:351-362. 2009

[9] Resende, Pedro Ernesto de et al. Uso dos basidiomicetos lentinus crinitus e lentinus strigosus como agentes descolorantes de efluentes de indústrias têxteis. Salão de Iniciação Científica (19.: 2007: Porto Alegre, RS). Livro de resumos. Porto Alegre: UFRGS, 2007., 2007.

[10] Bafana, Amit; Devi, Sivanesan Saravana; Chakrabarti, Tapan. Azo dyes: past, present and the future. Environmental Reviews, v. 19, n. NA, p. 350-371, 2011

[11] A.M. Zayed, M.S.M. Abdel Wahed, E.A. Mohamed, M. Sillanpää, Appl. Clay Sci. 166 (2018) 49.

[12] Hosseini, Soraya et al. Carbon coated monolith, a mesoporous material for the removal of methyl orange from aqueous phase: Adsorption and desorption studies. Chemical engineering journal, v. 171, n. 3, p. 1124-1131, 2011.

[13] Sousa, Paloma Viana Ferreira de. Preparo e avaliação do hidróxido duplo lamelar MgZnAl-Fe calcinado no processo de adsorção–fotodegradação do corante alaranjado de metila. 2015 [29] Lins, P.V.S., Henrique, D.C., Ide, A.H., Duarte, J.L. da silva, Dotto, G.L., Yazidi, A., Sellaoui, L., Erto, A., Zanta, C.L. de P. e. S., Meili, L., 2020. Adsorption of a non-steroidal antiinflammatory drug onto MgAl/LDH-activated carbon composite –Experimental investigation and statistical physics modeling. Colloids Surfaces A Physicochem. Eng. Asp. 586.

[14] Duarte Neto, João Fernandes et al. Processo de adsorção dos corantes alaranjado de metila e rodamina B por argilas esmectíticas da Paraíba, in natura e modificadas. 2015.

[15] D´Souza, E.; Fulke, A. B.; Mulani, N.; Ram, A.; Asodekar, M.; Narkhede, N.; Gajbhiye, S. N. Decolorization of Congo red mediated by marine Alcaligenes species isolated from Indian West coast sediments. Environmental Earth Sciences 2017 76,721

[16] Elmoubarki, R., Mahjoubi, F. Z., Elhalil, A., Tounsadi, H., Abdennouri, M., Sadiq, M., Qourzal, S., Zouhri, A., & Barka, N. (2017). Ni/Fe and Mg/Fe layered double hydroxides and their calcined derivatives: Preparation, characterization and application on textile dyes removal. Journal of Materials Research and Technology, 6(3), 271–283.

[17] Pérez-Ramírez, J., Mul, G., Kapteijn, F., & Moulijn, J. A. (2001). A spectroscopic study of the effect of the trivalent cation on the thermal decomposition behaviour of Co-based hydrotalcites. Journal of Materials Chemistry, 11(10), 2529–2536.

[18] Abderrazek, K., Srasra, N. F., & Srasra, E. (2017). Synthesis and Characterization of [Zn-Al] Layered Double Hydroxides: Effect of the Operating Parameters Kaouther Abderrazek. 346–353.

[19] Rodriguez-Rivas, F., Pastor, A., de Miguel, G., Cruz-Yusta, M., Pavlovic, I., & Sánchez, L. (2020). Cr3+ substituted Zn-Al layered double hydroxides as UV–Vis light photocatalysts for NO gas removal from the urban environment. Science of the Total Environment, 706, 136009.

[20] Li, M., Wu, G., Liu, Z., Xi, X., Xia, Y., Ning, J., Yang, D., & Dong, A. (2020). Uniformly coating ZnAl layered double oxide nanosheets with ultra-thin carbon by ligand and phase transformation for enhanced adsorption of anionic pollutants. Journal of Hazardous Materials, 397(February), 122766.

[21] Lobo-Sánchez, M., Nájera-Meléndez, G., Luna, G., Segura-Pérez, V., Rivera, J. A., & Fetter, G. (2018). ZnAl layered double hydroxides impregnated with eucalyptus oil as efficient hybrid materials against multi-resistant bacteria. Applied Clay Science, 153(October 2017), 61–69.